JOURNAL OF CATALYSIS 154, 379–390 (1995)

Adsorption and Thermal Decomposition of Methanol on the (100) Surface of NiAl: A Comparison to NiAl(110)

Bor-Ru Sheu and D. R. Strongin[1]

Department of Chemistry, State University of New York at Stony Brook, Stony Brook, New York 11794

Received October 5, 1994; revised February 7, 1995

The surface reactivity of the (100) plane of stoichiometric NiAl toward methanol has been investigated with temperature-programmed desorption (TPD), X-ray and ultraviolet photoelectron spectroscopy (XPS and UPS), and high-resolution electron energy loss spectroscopy (EELS). The atomic composition of the outermost surface of NiAl(100) is predominately Al, in contrast to the (110) plane of NiAl which is capped by an outermost layer that contains both Al and Ni. In an effort to understand the effects of the atomic composition of the surface on reactivity, results for CH_3OH/NiAl(100) are compared to prior results for CH_3OH/NiAl(110). Methanol chemisorption on both planes of NiAl, at 120 K, is primarily associative (some dissociation cannot be ruled out). Chemisorbed methanol transforms into surface methoxy in the temperature interval of 120 and 200 K on both NiAl(100) and NiAl(110). On the (110) surface, subsequent C–H and C–O bond breaking steps at higher temperatures lead to the evolution of gaseous H_2, CO, CH_4, CH_3 radicals, and small amounts of C_2H_4, in addition to the deposition of surface oxygen and carbon. The peak temperature of CH_4 desorption from NiAl(110) is near 350 K and the maximum rate of CH_3 radical desorption is located at 570 K. In contrast, methoxy decomposition on the NiAl(100) surface generates a much smaller amount of CH_4 and the reaction channel leading to gaseous CO is completely suppressed. The presence of Ni atoms in the top layer of the (110) surface is suspected to be responsible for both CH_4 and CO production on NiAl(110).

1. INTRODUCTION

Reactions taking place on an alloy are profoundly influenced by the atomic composition of the surface layer (1). Investigation of this influence is often complicated by the difficulty in elucidating the composition and structure of the bimetallic surface in detail. This problem is alleviated to some extent for the NiAl alloy, since the low index surface planes of this material have a well-defined surface composition and structure. For example, the NiAl(110) surface exhibits an atomic composition (which consists of equal amounts of Ni and Al) and structure that are similar to what one would predict by assuming an ideal termination of the bulk. The structure of the NiAl(100) surface also is similar to the corresponding bulk plane, but unlike NiAl(110) the atomic composition of the terminating layer of this plane can be either Al or Ni (2, 3). It has been shown experimentally that the (100) surface plane is capped by an Al layer (4). We are of the opinion then that NiAl provides a useful model system for the study of the relationship between the surface reactivity and atomic composition of alloy surfaces. Also, from a more practical standpoint the investigation of the surface reactivity of NiAl may have relevance to the understanding of catalysts composed of Ni supported on oxidized Al (5).

In this contribution we investigate the reactions of CH_3OH on the (100) plane of NiAl in the ultra-high vacuum environment and compare our results to prior research of the chemisorption and reaction of CH_3OH on NiAl(110) (6). It was shown in the prior work that cleavage of the C–O bond of $CH_3O_{(ad)}$, which results from CH_3OH reaction, occurs between 300 and 400 K on NiAl(110). Some of this decomposing $CH_3O_{(ad)}$ results in the desorption of gaseous methane, but the majority of this intermediate results in the deposition of carbonaceous species and surface oxygen. At higher temperatures gaseous CO and CH_3 radicals form and extensive hydrogen evolution occurs. With regard to the C–O bond cleavage between 300 and 400 K, it might be inferred that both Ni and Al are intimately involved, given that this temperature interval is lower than what has been observed for the breaking of the C–O bond of $CH_3O_{(ad)}$ on monometallic Al (7–11). Furthermore, the production of CO from the decomposition reactions of $CH_3O_{(ad)}$ occurs on Ni (12–29) (and Ni/Al_2O_3 (30)) but not on Al surfaces (7, 8). The reaction of CH_3OH on NiAl(100) provides an interesting contrast, since the Ni resides underneath the outermost Al layer (4). A goal of the research reported in this paper is to investigate whether decomposition channels, present on NiAl(110), for the decomposition of $CH_3O_{(ad)}$ (namely, low-temperature C–O scission and CH_4 evolution, and

[1] To whom correspondence should be addressed. E-mail:dstrongin@sbccmail.

0021-9517/95 $12.00

CO production) are available on the (100) plane, where only Al is present in the outermost surface of the clean surface. Furthermore, the effects of the surface atomic composition on the initial chemisorption of CH_3OH on NiAl is of interest and will be addressed.

We show in this article that CH_3OH adsorbs on NiAl(100), primarily in an associative manner near 120 K, resulting in a layer of $CH_3OH_{(ad)}$. Upon heating to 200 K all of the CH_3OH converts to $CH_3O_{(ad)}$, and further heating to 300 K begins to decompose the methoxy overlayer. In contrast to the CH_3OH/NiAl(110) system, the production and desorption of CO is not observed to occur on NiAl(100). In addition, only a relatively small amount of CH_4 is produced on NiAl(100) via methanol decomposition, compared to NiAl(110). These two experimental results suggest that the presence of Ni atoms in the outermost layer facilitates the production of both CO and CH_4 product. Heating $CH_3O_{(ad)}$ in the temperature interval of 500 and 600 K results in the desorption of methyl radicals and methane. The reaction channel that produces methyl radical between 500 and 600 K appears to be similar on both the (110) and the (100) planes of NiAl, by virtue of this product showing a similar peak temperature during temperature-programmed desorption (TPD) experiments on both planes.

2. METHODS

All the experiments discussed in this paper were carried out in a two-level stainless steel ultra-high-vacuum (UHV) chamber with a typical working pressure of 2×10^{-10} Torr. Surface sensitive techniques which could be carried out in the UHV chamber, were TPD, low-energy electron diffraction (LEED), ultraviolet and X-ray photoelectron spectroscopy (UPS and XPS), and high-resolution electron energy loss spectroscopy (EELS).

The cleaning procedure for the NiAl(100) crystal (8 mm $\times$ 8 mm square and 2 mm thick) was similar to what has been described in detail for the (110) plane in a prior publication (6). Briefly, the cleaning of the samples was accomplished by repeated 500-eV argon ion sputter and anneal (1150 K for 20 min) cycles. A trace amount of carbon was removed by heating the NiAl crystals in 1×10^{-7} Torr of oxygen at 1000 K. Sharp (1×1) LEED patterns were obtained for both NiAl(110) and NiAl(100) after this cleaning procedure. Samples were mounted by spot-welding 3 Ta wires (0.025 cm diameter) to each side of the sample. The ends of the support wires were then spot-welded to Ta tabs that were attached to a liquid nitrogen cryostat. This mounting allowed the samples to be cooled to 120 K, and by passing current through the support wires the samples could be rapidly heated to 1300 K.

The methanol (CH_3OH, HPLC grade, Fisher Chemical; CD_3OD, > 99.8 atom% D, Cambridge Isotope Laboratories; CD_3OH, 99 atom% D, Aldrich Chem. Co.) used in this study was purified by numerous freeze–pump–thaw cycles. Exposure of the sample to methanol was accomplished by translating the sample to within 5 mm of a 0.05-cm-diameter dosing tube that was connected to a leak valve. The methanol exposures quoted in this paper (in Langmiurs = 10^{-6} Torr sec) are our best estimates, after correcting for both the dosing geometry and for the sensitivity of the ionization gauge that was used to measure the gas pressure.

TPD experiments were performed with a 7 ± 1 K/sec heating rate. The mass spectrometer used for these experiments was multiplexed so that all the desorbing species could be identified in a single experiment as a function of temperature. Relative yields of gaseous products quoted in this paper have been calculated in view of the mass spectrometer sensitivities for the different desorbing species (determined by using reference sample gases). The mass spectrometer was housed in a gold-plated stainless steel enclosure with a 5-mm-diameter aperture. A chromel–alumel (type K) thermocouple wire was spot-welded to the top of the NiAl samples for temperature measurements.

Photoelectrons emitted from the sample during UPS and XPS were analyzed with a double-pass cylindrical mirror analyzer. He I (21.2 eV) and MgKα (1253.6 eV) radiation were used for the UPS and XPS experiments, respectively. The CMA was set for a pass energy of 5 and 50 eV for the UPS and XPS measurements, respectively. All binding energies presented in this paper are given relative to the sample Fermi level (E_F). Work function changes ($\Delta\phi$, ± 0.3 eV uncertainty, 4 V sample bias) reported in this contribution were obtained by analyzing the change in the secondary electron cutoff during UPS measurements.

All EELS data were acquired at a specular detection angle ($\theta_i = \theta_f = 60°$) with a primary beam energy of 3.5 eV. A typical counting rate of 10^4 Hz and a resolution of 96 cm^{-1} (FWHM) were measured for the elastically scattered electrons from NiAl(110) and NiAl(100). The resolution and counting rate of the primary beam varied from 100 to 140 cm^{-1} and from 5×10^2 to 5×10^3 Hz, respectively, after exposure of NiAl crystals to methanol. The vibrational frequencies reported in this paper reproduce to within ±10 cm^{-1} from run to run.

3. RESULTS AND DISCUSSION

TPD, XPS, UPS, and EELS results are presented in this section for the adsorption and reaction of CH_3OH on the (100) and (110) planes of NiAl. The subsections are set up by technique and in each one of these subsections results for both planes of NiAl are presented and con-

trasted. We mention that results for CH_3OH on NiAl(110) are discussed in detail elsewhere (6). In view of this circumstance this paper details new results for CH_3OH/NiAl(100) and selected results for CH_3OH/NiAl(110) will be presented as a comparison to the (100) plane.

3.1. Product Desorption from CH_3OH/NiAl(100) and CH_3OH/NiAl(110)

Figures 1a and b show desorption traces for species that desorb from the (100) and (110) planes of NiAl after exposure to 6 and 5.4 L of CH_3OH, respectively (the sharp peak near 150 K in most of the spectra is due to the desorption of CH_3OH from a multilayer). Inspection of Fig. 1a shows that H_2 (m/e = 2), C_2H_4 (m/e = 27 and 28), and CH_3 radicals (m/e = 15) desorb from NiAl(100) after exposure to CH_3OH. CH_4 (m/e = 16) is also detected during TPD for CH_3OH/NiAl(100), but much of this signal is indirectly due to methyl radical desorption and is discussed later. (We note that at our mass spectrometer settings the cracking of CH_4 yields an m/e = 16 : 15 ratio of 1.2, indicating that the m/e = 15 signal in Fig. 1a cannot be due solely to the cracking of CH_4.) Fig. 1b shows analogous TPD data for the NiAl(110) face. One difference to note, however, is that unlike part (a) of the figure, the m/e = 15 spectrum for CH_3OH/NiAl(110) is obtained by subtracting the CH_3^+ intensity, which is due to fragmentation of CH_4, from the raw CH_3^+ intensity. The resulting difference curve, therefore, is due to the desorption of a product other than CH_4.

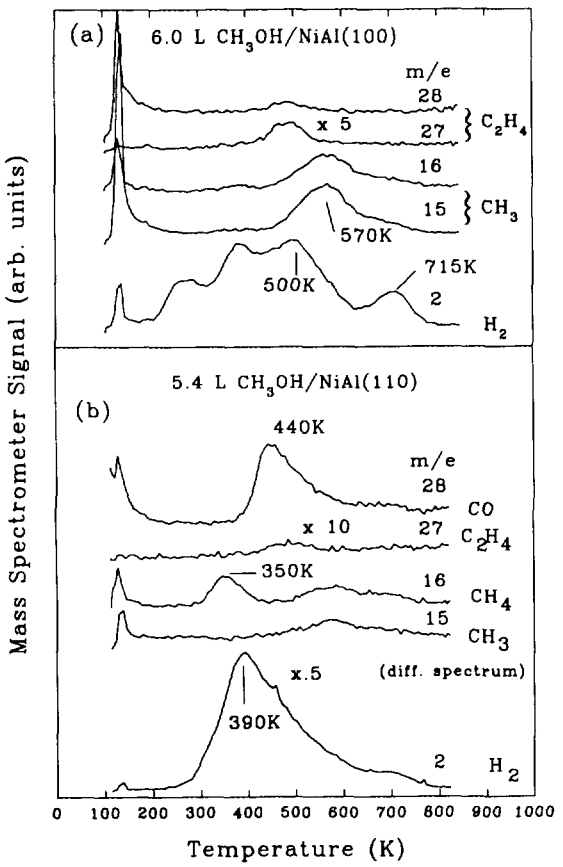

FIG. 1. Products desorbing from (a) NiAl(100) and (b) NiAl(110) after exposure to 6 and 5.4 L of CH_3OH, respectively. The sharp desorption feature near 150 K is associated with the desorption of CH_3OH from a condensed layer. The (110) spectra, in contrast to those for the (100) plane, show CO desorption in addition to a greater amount of CH_4 desorption at low temperature (~350 K). Both CO and low temperature CH_4 production are thought to be facilitated by the presence of Ni in the outermost surface of NiAl(110). Note that the m/e = 15 spectrum for CH_3OH/NiAl(110) is a difference spectrum (see text).

Perhaps, the most significant difference between the (110) and (100) faces is that CO (m/e = 28) and CH_4, with peak maxima of 440 and 350 K, respectively, appear prominently in the product distribution for NiAl(110) but not for NiAl(100). Only a small amount of CH_4 desorption is experimentally observed desorbing from NiAl(100) near 350 K, and this occurs only after high CH_3OH exposures. Similarities with regard to product distributions, however, exist between the TPD data for the two faces. Possibly, the most noticeable of these is that H_2 and CH_3 radicals appear as products for both surface, in addition to a much smaller amount of C_2H_4.

The identification of CH_3 radical products is quite indirect and it is probably worthwhile to briefly discuss this assignment. As mentioned above, Fig. 1b exhibits an m/e = 15 difference spectrum, which is obtained by subtracting the contribution of CH_3^+, which is due to the cracking of CH_4 in the ionizer of the mass spectrometer,[2] from the raw m/e = 15 signal. A similar difference spectrum, while not shown, can be obtained for CH_3OH/NiAl(100). In either case, the 570 K peak in the m/e = 15 difference spectra cannot be due to CH_4. We postulate instead, based largely on this observation, that these desorption features are due to methyl radicals. Other experimental observations also lend support to this contention and this is discussed, in context of the CH_3OH/NiAl(110) system, in a prior publication (6).

Examination of Fig. 2, which exhibits m/e = 18, 19, and 20 TPD traces for CD_3OD/NiAl(100), suggests that some CH_4 is desorbing in addition to the methyl radicals near 570 K. The first thing to notice is that the m/e = 18 peak (CD_3^+) near 570 K is more intense than the corresponding features at or near 570 K in the m/e = 19 and 20 spectra. Thus, all of the peak intensity near 550 K in the m/e = 18 spectrum cannot be attributed to CD_4 desorption from the (100) crystal and subsequent ioniza-

[2] The cracking pattern of methane at an electron impact energy of 70 eV, using our mass spectrometer, has been measured to be 100 : 87 : 15 for m/e 16 : 15 : 14.

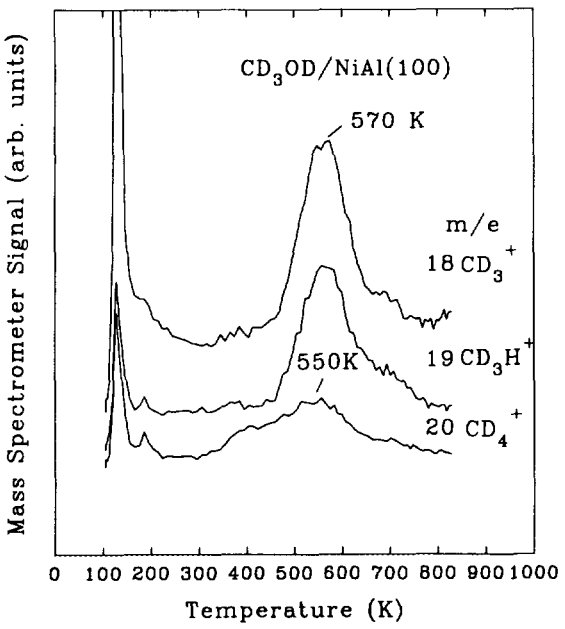

FIG. 2. Desorption traces of CD_4, CD_3, and CD_3H for CD_3OD/NiAl(100). We believe that CD_3H results from the desorption of CD_3 from the NiAl(100) sample and the subsequent abstraction of hydrogen from the walls of the experimental chamber, prior to detection by the mass spectrometer. Some CD_4 is formed on the sample surface, as shown by the CD_4^+ curve, which has a peak maximum at a temperature that is about 20 K lower than that of CD_3 (or CD_3H) product.

tion in the mass spectrometer. Instead, we associate some portion of this m/e = 18 desorption feature with the desorption of CD_3 radicals. The intensity at 570 K in the m/e = 19 spectrum is also associated with the desorption of CD_3 from the NiAl(100) surface, but in this case we suspect that the methyl radical is converted to CD_3H via collisions (i.e., $CD_3 + H_{(ad,wall)} \rightarrow CD_3H$) with surfaces within the mass spectrometer shield, prior to detection (33–35).[3] The 550 K feature in the m/e = 20 spectrum shows a downward shift of about 20 K, with respect to the m/e = 18 and 19 features near 570 K. This m/e = 20 feature is thought to be due to the desorption of CD_4 from the NiAl(100) surface during the decomposition reactions of CD_3OD. Notice that the m/e = 20 spectrum also exhibits a relatively weak feature near 400 K, which we suspect is analogous to the ~400 K CD_4 feature that is observed in the corresponding TPD trace for CD_3OD/NiAl(110) (6). The yield of CD_4 or CH_4 resulting from CD_3OD or CH_3OH decomposition, however, is much greater from the (110) plane than from the Al-terminated (100) plane, as will be quantified later.

[3] The hydrogen abstraction reaction of methyl radicals in the experimental chamber has also been reported by other laboratories to be a serious problem in the quantitiative detection of methyl radicals. See Refs. (33–35) for examples.

H_2 traces for NiAl(100) after various exposures of CH_3OH are shown in Fig. 3a. At the lowest exposure there are two broad features near 250 and 500 K. With increasing exposure, these two features grow in intensity and at least two more features grow in intensity at about 390 and 715 K. The highest temperature peak also appears in H_2 traces for CH_3OH/NiAl(110) at a similar temperature, and we believe this desorption state is due to the decomposition of carbonaceous fragments on a predominately aluminum oxide surface layer. Hydrogen desorption from NiAl(100), above 400 K, is presumably not controlled by the desorption kinetics of surface-bound hydrogen but instead by the kinetics of C–H bond cleavage steps. We support this statement with desorption traces of H_2, HD, and D_2 for CD_3OH adsorbed on NiAl(100), which are shown in part (b) of Fig. 3. Desorption of H_2, originally located in the O–H bond of CD_3OH, exhibits a peak maximum of 260 K, and its desorption is complete by 400 K. We show in the next section that O–H bond cleavage occurs at temperatures as low as

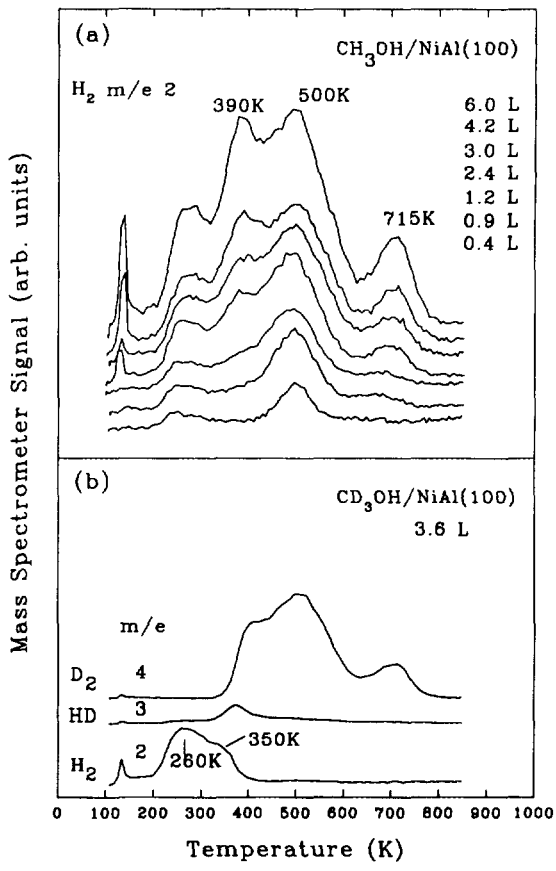

FIG. 3. (a) H_2 traces for CH_3OH/NiAl(100) as a function of CH_3OH exposure. (b) H_2, HD, and D_2 traces for CH_3OD/NiAl(100). Not much HD is experimentally observed, suggesting that the desorption of hydrogen, originally in the hydroxyl group of CD_3OH, occurs before C–D bond cleavage occurs (≥400 K).

150 K on NiAl(100), implying that H_2 desorption is controlled by the kinetics of adsorbed hydrogen. The D_2 desorption profile suggests that C–D bond cleavage begins to occur at temperatures near 400 K.

Little HD desorption from NiAl(100) is experimentally observed, suggesting that the combination and desorption of H_2 is complete by the temperature at which C–D bond cleavage initiates. Much more isotope mixing occurs between the hydroxyl and methyl hydrogen when methoxy decomposes on NiAl(110) (6). This mixing on NiAl(110) can probably be explained by noting that on NiAl(110), the onset of hydrogen desorption, resulting from C–H bond cleavage, begins at 300 K. Surface hydrogen, resulting from O–H bond cleavage is still present on the reacting surface at these temperatures, as evidenced by the fact that D_2 desorption from CH_3OD decomposition on the (110) face occurs with a peak temperature of 350 K ($H_{2(g)}$ resulting from O–H bond cleavage occurs at the same temperature) (6). Therefore, in contrast to CH_3OH/NiAl(100), hydrogen resulting from both methyl and O–H bond cleavage is present on the NiAl(110) surface over a common temperature interval allowing rapid mixing to occur.

It is not entirely clear why H_2, resulting from low-temperature O–H bond cleavage, desorbs at a higher temperature from NiAl(110) than from NiAl(100). Electronic differences between the two faces ultimately determine the differences in hydrogen binding on the two surfaces. Nevertheless, the atomic composition of the surface is important, and it is noted that hydrogen desorbs from the Al-terminated surface (i.e., NiAl(100)) at lower temperatures than it does from the (110) surface, which has both Ni and Al in it. Ni binds hydrogen more strongly than Al, and it might be that the presence of Ni in the outermost layer holds hydrogen on the surface upto higher temperatures. This simple explanation is not entirely satisfactory since hydrogen often can bond to second layer atoms and/or penetrate deeper into the subsurface region. Thus, even in the NiAl(100) circumstance, it might be expected that hydrogen could interact strongly with the Ni component. With regard to this possibility, it is interesting to note that in addition to the major H_2 desorption feature at ~260 K for CH_3OH/NiAl(100), there is a second feature (a shoulder) with a maximum near 350 K. This additional feature may be due to hydrogen desorbing from sites with a strong influence from Ni, in view of the fact that the corresponding desorption feature for CH_3OH/NiAl(110) occurs at a similar temperature.

Before we proceed to the presentation of electron spectroscopy results, it is useful to summarize some of the TPD results. First, we postulate on the basis of the desorption data that the surface crystallographic structure is an important factor in controlling the type and desorption kinetics of products that desorb from the surfaces of the NiAl alloy during the decomposition reactions of CH_3OH. Production of CO and CH_4 appear to be facilitated by the presence of Ni atoms in the reacting surface since in contrast to the (110) plane no CO and a relatively small amount of CH_4 is produced on NiAl(100), which is terminated by an Al layer. On the other hand, CH_3 groups are evolved from both crystal faces at a similar peak temperature. By virtue of this similarity, it is suspected that similar reaction steps lead to the formation of this product on both NiAl alloy surfaces. It is mentioned that in the temperature range of 500–600 K, where methyl groups desorb, the surface of both crystal faces is presumably highly oxidized and enriched in Al, with respect to the clean surfaces. We feel then that the production of methyl radicals occurs on a surface that is predominately composed of Al or its oxide.

3.2. XPS Results and Estimation of Gaseous Product Yields

Figure 4 exhibits O(1s) and C(1s) XPS data obtained after exposure of NiAl(100) to 6 L of CH_3OH at 120 K and heating to the indicated temperatures. All the assign-

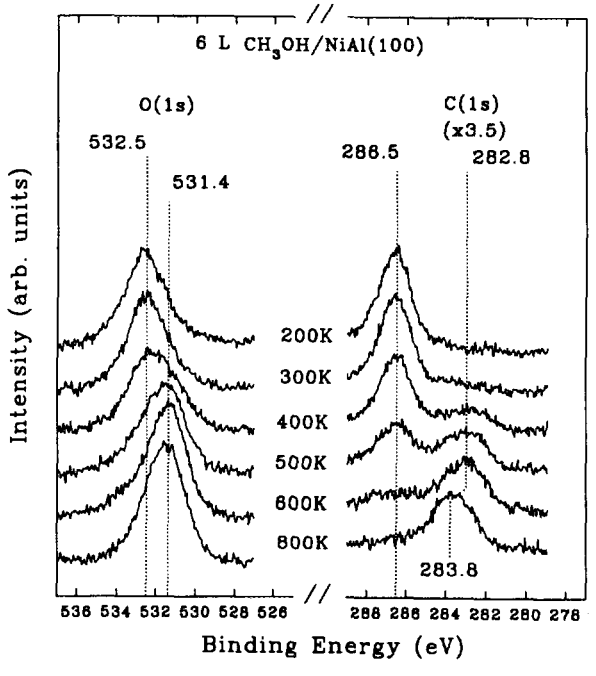

FIG. 4. O(1s) and C(1s) XPS spectra of methoxy on NiAl(100) at 200 K and after stepwise heating to various temperatures. Preparation of the methoxy adlayer at 200 K is carried out by heating a CH_3OH multilayer on NiAl(100) at a temperature of 120 to 200 K. The O(1s) and C(1s) peaks at 532.5 and 286.5 eV are associated with $CH_3O_{(ad)}$, and the features that evolve with temperature at 531.4 and 282.8 eV are attributed to surface oxygen and carbonaceous fragments that result from methoxy decomposition.

ments for the features that appear in these spectra have been discussed in detail in previous publications with regard to other 3d-transition metal aluminide surfaces (6, 34). Briefly, O(1s) and C(1s) features that appear at 532.5 and 286.5 eV, respectively, are associated with adsorbed $CH_3O_{(ad)}$. (The presence of methoxy on NiAl(100) at 200 K is well supported by vibrational and valence band spectroscopy in the following sections.) Spectral features that progressively evolve, at 531.4 and 282.8 eV in the temperature interval of 200 and 800 K, at the expense of the spectral weight due to methoxy, are associated with surface oxygen (presumably bound to Al) and carbonaceous species. We do not know for sure but it is thought that the shift of the C(1s) feature from 282.8 to 283.8 eV is due to extensive oxidation and restructuring of the NiAl(100) surface, thus changing the chemical environment of the carbonaceous species.

In contrast to the forthcoming EELS and UPS data, XPS measurements allow the amounts of methoxy, surface-bound oxygen, and carbon-containing decomposition fragments, at various temperatures, to be estimated on the basis of O(1s) and C(1s) peak areas.This peak area data is plotted in Figs. 5a and 5b, along with complimentary data for NiAl(110). Note that we have normalized the peak area for the O(1s) and C(1s) features of methoxy on NiAl(100) and NiAl(110) at 200 K to a value of 100. The area of the O(1s) peak for methoxy on NiAl(100) and NiAl(110), shown in Fig. 5a, remains unchanged, within experimental error, upon heating to 400 K. Heatjying to 500 K and higher results in no signficant O(1s) peak area change for the NiAl(100) surface. Thermal annealing of the (110) plane to 500 K, however, results in an 11% decrease in the O(1s) intensity, which we attribute to the desorption of CO. Heating to 800 K results in no further change in the amount of oxygenated species on NiAl(110).

O(1s) data is only given as a total area since unambiguous deconvolution of the O(1s) peak, into contributions from methoxy and surface oxygen, is not possible. C(1s) data shown in Fig. 5b, however, allows us to separate the relative concentration of methoxy and carbonaceous fragments over the whole heating interval. The peak area due to the C(1s) feature of methoxy (i.e., at 286.5 eV) on both NiAl(100) and NiAl(110) begins to decrease after heating to 400 K and continues to drop sharply upon heating to 500 K. This decrease in the methoxy peak area is paralleled by increases in the peak intensity due to carbonaceous decomposition fragments (i.e., at 282.8 eV). The plotted points for the total C(1s) area, however, show that more carbon is removed from the NiAl(110) surface upon heating from 300 to 500 K than is removed from NiAl(100). We attribute this difference to the desorption of CH_4 from NiAl(110) in the temperature interval of

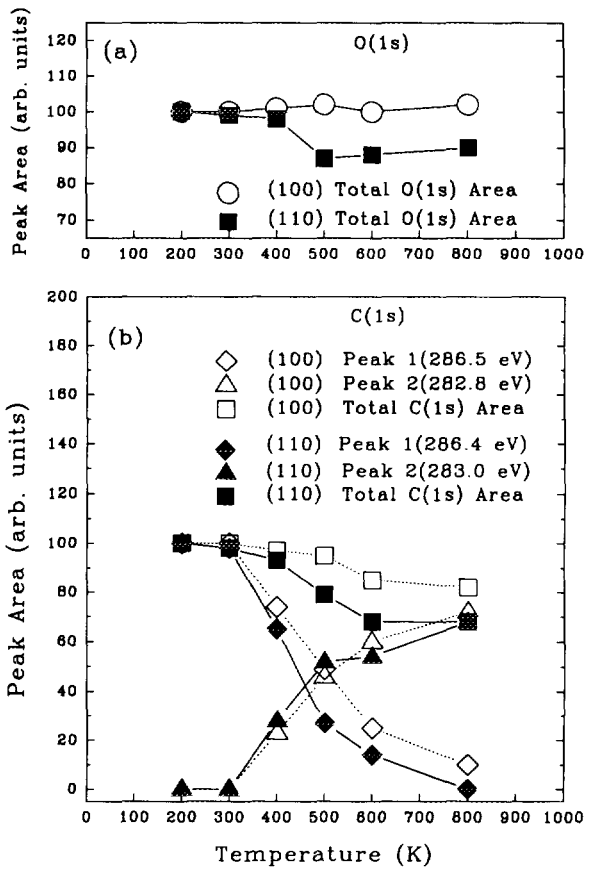

FIG. 5. Plot of the (a) O(1s) and (b) C(1s) peak areas vs temperature for the CH_3OH/NiAl(100) and CH_3OH/NiAl(110) systems. The total O(1s) area for CH_3OH/NiAl(110) decreases between 400 and 500 K and this is due to the desorption of CO. Part (b) of the figure shows that the total C(1s) peak area for CH_3OH/NiA(110) is less then that of CH_3OH/NiAl(100) after it is annealed to 600 K. This difference is due to the production and desorption of CO from the (110) plane, in addition to the enhanced yield of CH_4 relative to the Al-terminated (100) surface.

300 to 400 K and to the evolution of CO product from the (110) face in the temperature interval of 400 to 500 K. The total C(1s) peak area for both surfaces shows a further decrease upon heating from 500 to 600 K, and this is attributed, at least in part, to the desorption of CH_3.

These XPS data, in conjunction with the sensitivities of the mass spectrometer for the individual gases, allows us to give the yield of each reaction product that desorbs from the (100) and (110) planes of NiAl after similar exposures of CH_3OH (see Fig. 1) in terms of a percent of the initial methoxy coverage at 200 K. We can infer from the data in Fig. 6, for example, that the decomposition of an amount of methoxy, equal to 15% of the initial adlayer at 200 K on either NiAl(100) or NiAl(110), occurs in parallel with the desorption of CH_3 radicals. Note that the data do not allow us to quantitatively compare the yield of a given product for the CH_3OH/NiAl(100) against that same

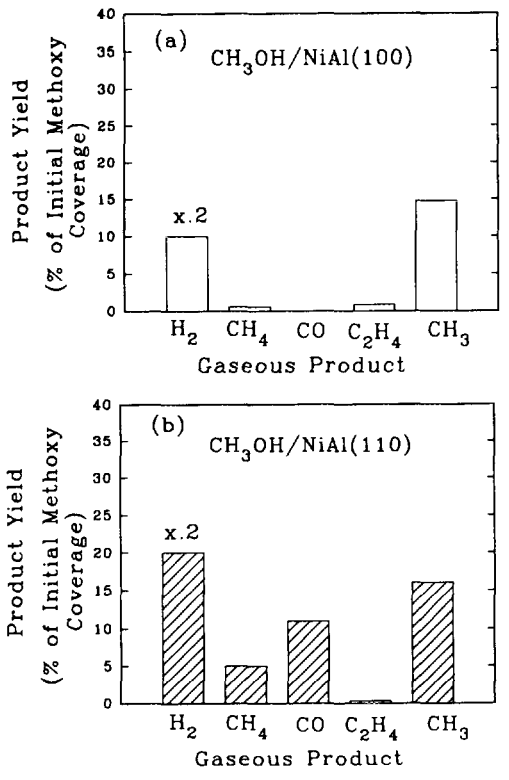

FIG. 6. Comparison plot of the product yields for CH_3OH/NiAl(100) and CH_3OH/NiAl(110). Perhaps the greatest difference in yields is that the (110) plane produces CO and greater amounts of CH_4 during the decomposition reactions of CH_3OH.

product yield for the CH_3OH/NiAl(110) surface.[4] Qualitatively, however, we can safely say that CO is only produced on the (110) plane and CH_4 production is much more facile on this surface then on the (100) plane. Also, the amount of surface hydrogen, resulting from the decomposition of $CH_3O_{(ad)}$ on NiAl(110), that desorbs as molecular hydrogen is estimated to be two times greater than the amount of H_2 that desorbs from the (100) plane of the alloy surface. Presumably, much of the surface hydrogen on the NiAl(100) surface, which results from $CH_3O_{(ad)}$ decomposition, becomes trapped in the aluminum oxide layer (shown later by EELS) that forms.

[4] To obtain an accurate comparison of the yields between the two surfaces, two points concerning the TPD and XPS results must be addressed. First, the area of the sample that is observed during CH_3OH/NiAl(100) and CH_3OH/NiAl(110) TPD needs to be the same. We feel that this requirement is met for our experiment, due to the mass spectrometer shield construction. The second point is that the relative coverage of methoxy on the two different planes of NiAl is needed. We find that the ratio of C(1s) areas for methoxy on the NiAl(100) and NiAl(110) planes is 0.7, suggesting that the coverage of methoxy on the former surface is greater than on the latter. We are not sure how reliable this result is, due to differences in sample sizes and slight differences in the sample position during XPS measurements; we therefore refrain from comparing yields in detail.

3.3. Methanol-Exposure and Annealing-Temperature Dependence of EELS Spectra

Previous research of the (110) face of NiAl suggests that CH_3OH, for the most part, adsorbs in an associative manner (6), and EELS data presented in this section suggest that the gross adsorption behavior of CH_3OH on the (100) plane is similar. Before the EELS data is reviewed, it is worthwhile to review the TPD data in Fig. 7. These data show that CH_3OH does not desorb from the (100) face at CH_3OH exposures of 2.4 L or less. At exposures higher than 2.4 L a sharp CH_3OH desorption feature appears near 150 K, which is assigned to sublimation of a condensed molecular layer. We conclude from these data that exposures less than 2.4 L of CH_3OH result in adsorbate coverages where most of the species are interacting directly with the NiAl(100) alloy surface. With this result in mind the EELS data are now presented.

Figure 8 exhibits EELS data of NiAl(100), as a function of CH_3OH exposure at 120 K. A 10 L CH_3OH exposure results in the formation of a condensed layer and the vibrational modes in the corresponding EELS spectrum can be readily assigned. The 2985 cm^{-1} and 1475 cm^{-1} bands are assigned to C–H stretching and CH_3 deformation modes, respectively, and the 3260 and 765 cm^{-1} bands are assigned to O–H stretching and O–H bending modes, respectively. The features at 1070 and 1150 cm^{-1} are assigned to C–O stretching and CH_3 rocking modes, respectively. The 6.0-L spectrum exhibits an additional loss feature at 610 cm^{-1} and we assign this mode to the metal–oxygen stretch of adsorbed methanol. This loss feature is also present in the 0.8 and 1.6 L spectra and

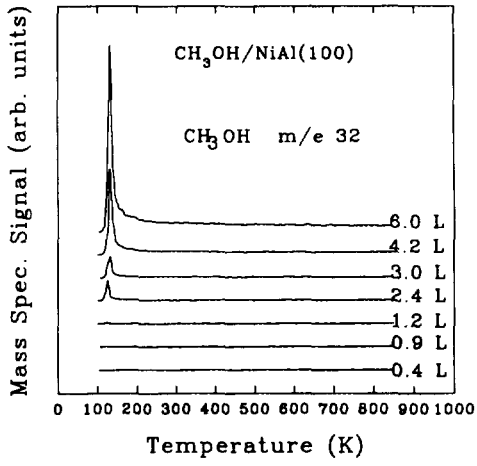

FIG. 7. CH_3OH traces for NiAl(100) that has been exposed to various amounts of CH_3OH. An exposure of 2.4 K results in the appearance of a sharp peak at 150 K, which is associated with the desorption of CH_3OH from a condensed layer. We infer from these data that at exposures greater than 1.2 and less than 2.4 L a CH_3OH multilayer begins to form.

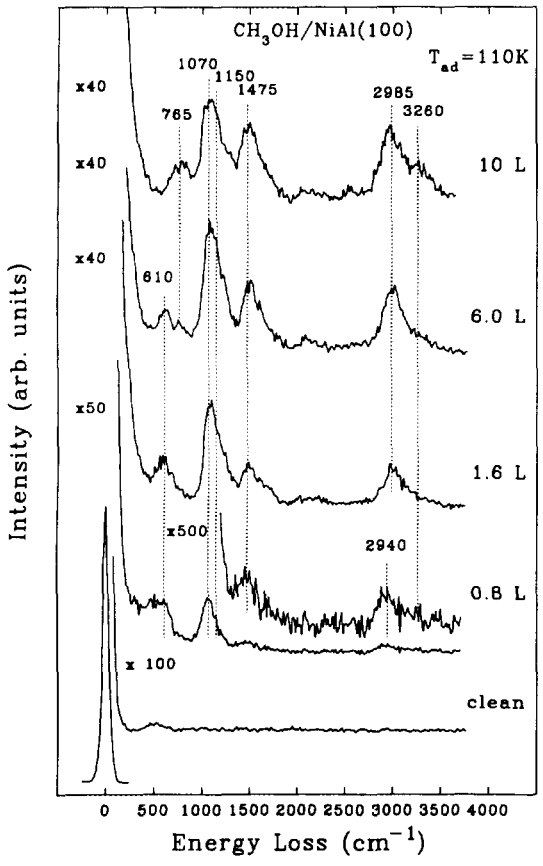

FIG. 8. EELS spectra of CH_3OH/NiAl(100) as a function of CH_3OH exposure.

the constancy of the frequency of this mode with coverage suggests that a similar chemical species exists at these different converages. Largely because of the presence of this mode at different coverages, we propose that at 120 K, CH_3OH adsorbs associatively on NiAl(100) at these relatively high CH_3OH exposures. This assignment is somewhat ambiguous since clearly defined O–H bending and stretching (expected to be near 765 and 3250 cm^{-1}) modes are absent from the EELS spectrum. We attribute this absence to a low-scattering cross section and/or an adsorption geometry that results in these modes being dipole forbidden. Weak O–H related modes are not inconsistent with other studies of chemisorbed CH_3OH on surfaces. Nevertheless, we will offer UPS results that support this claim of associative adsorption. It is emphasized, however, that partial dissociation of CH_3OH to $CH_3O_{(ad)}$ cannot be ruled out.

Figures 9a and 9b exhibit EELS data of CH_3OH adsorbed on NiAl(100) and NiAl(110) and of these systems after heating to various temperatures. The 110 and 120 K spectra for the (100) and (110) faces, respectively, are representative of a CH_3OH multilayer. We first discuss data for the CH_3OH/NiAl(100) system. As alluded to before, the 110 K CH_3OH/NiAl(100) spectrum exhibits an energy loss feature at 610 cm^{-1} that is presumably due to the metal–oxygen stretch of adsorbed CH_3OH. Heating to 150 K removes the multilayer, and the major differences between the 110 and 150 K spectra are that the higher temperature vibrational data exhibit a mode at 640 cm^{-1} and an increase in the intensity ratio of the C–O stretching mode at 1070 cm^{-1} to the modes associated with the vibrations of the hydrocarbon functional group. Heating to 200 K results in a spectrum that is indistinguishable from the 150 K spectrum. We first postulate that the 640 cm^{-1} mode is associated with the metal–O stretch of an adsorbed $CH_3O_{(ad)}$ species, and hence, O–H bond cleavage occurs by 150 K. The absence of any O–H vibrational modes certainly supports this assignment but does not prove it, since we already concluded from data in Fig. 8 that the O–H modes appear to be very weak in intensity. Better support for this assignment is probably obtained by noting that this mode at 640 cm^{-1} persists in position and intensity upon heating to 300 K, where TPD has already shown that the majority of hydroxyl-hydrogen has already desorbed. Heating to 800 K in a stepwise fashion results in the progressive decomposition of $CH_3O_{(ad)}$ (i.e., C–O bond cleavage occurs), as evidenced by the continual decrease in the C–O stretching and hydrocarbon modes. It is mentioned that the vibrational modes, for the most part in the 600 K spectrum and entirely in the 800 K spectrum, are associated with aluminum oxide.

Part (b) of the same figure displays complimentary data for $CH_3O_{(ad)}$ on NiAl(110) at 200 K and after heating to temperatures similar to those used for exploring the thermal stability of methoxy on the (100) plane. Comparison of the EELS data suggests that the decomposition intervals of methoxy on the (110) and (100) planes are quite similar. For example, the 400 K spectra for both alloy surfaces show the presence of the 780 cm^{-1} mode, which we associate with surface oxygen bound to the Al component (resulting from the partial decomposition of $CH_3O_{(ad)}$). Also, data for both surfaces show that substantial decomposition of methoxy occurs between 400 and 500 K, as judged by the decrease in the ν(C–O) mode near 1040 cm^{-1}. Heating either CH_3OH/NiAl(100) or CH_3OH/NiAl(110) to temperatures near 600 K or above results in EELS spectra that show intense loss modes below 1000 cm^{-1}, which are associated with an aluminum oxide layer. Even though the EELS results suggest that the thermal stability of methoxy is similar on the (100) and (110) planes, the vibrational data show that the binding geometry of the intermediate is different on the two surfaces. One difference is that the ν(M–O) mode of $CH_3O_{(ad)}$ on NiAl(110) is at 540 cm^{-1}, a red shift of 100–110 cm^{-1} with respect to the NiAl(100) surface. This difference is ascribed to dissimilar binding environments for $CH_3O_{(ad)}$ on the Al-terminated (100) surface and the (110) surface,

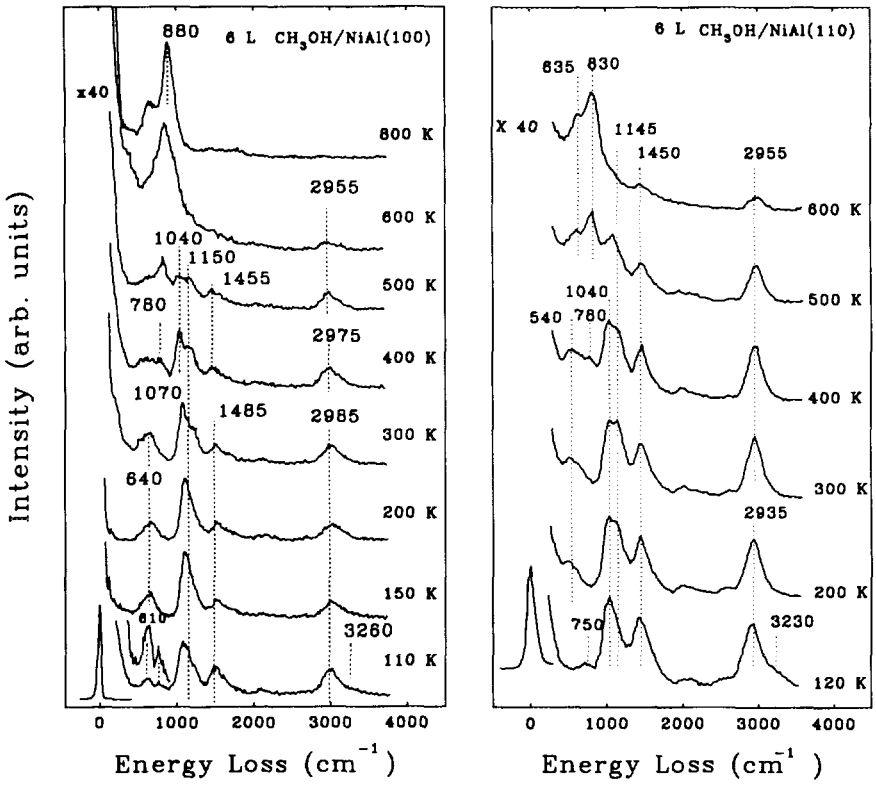

FIG. 9. Comparison of EELS data for the CH_3OH/NiAl(100) and CH_3OH/NiAl(110) systems as a function of temperature. In each circumstance a CH_3OH multilayer is condensed on the relevant NiAl surfaces (at 110 K for NiAl(100) and at 120 K for NiAl(110)) and then the CH_3OH/NiAl surface is heated in a stepwise fashion to various temperatures. The spectra are obtained at a temperature at or below 120 K.

which is capped by both Ni and Al atoms. A second difference is that the ν(C–O) to ν(C–H) mode intensity ratio for $CH_3O_{(ad)}$ on NiAl(100) is significantly greater than the corresponding ratio of modes when $CH_3O_{(ad)}$ is adsorbed on the (110) plane. We briefly discuss these points later in the context of our other electron spectroscopy and desorption results.

3.4. UPS of CH_3OH/NiAl(110) and CH_3OH/NiAl (100)

UPS data on NiAl(100) after exposure to 1.2 L of CH_3OH at 120 K and after stepwise heating to various temperatures are exhibited in Fig. 10. Note that the spectra are presented as difference curves (i.e., clean NiAl(100) data has been subtracted from CH_3OH/NiAl(100) data). Consistent with at least some CH_3OH associatively adsorbing on 110 K, there are four broad features present in the corresponding UPS spectrum that are characteristic of molecular CH_3OH. In order of increasing binding energy, they are located at 6.5, 8.2, 10.5, and 12.6 eV below E_F, which we associate with the 2a", 7a', 1a"/6a', and 5a' orbitals of chemisorbed CH_3OH (note that the ionization potentials of these levels in gas-phase CH_3OH[38] are marked by vertical lines at the top of the figure). While not shown here, we find that exposure of NiAl(100) to CH_3OH results in a decrease in the clean surface work function until an exposure near 2.5 L, at which the work function reaches a plateau value of 3.0 eV (presumably a CH_3OH multilayer begins to form), which translates into a work function change of -1.6 eV. This behavior is very similar to what we have found for CH_3OH on the (110) plane of NiAl (6). Exposure of NiAl(100) to 1.2 L results in a 1.0 eV decrease in work function. Taking this result in view of the TPD results that show no CH_3OH desorbing below a 2.4 L exposure, we conclude that exposure of the alloy to 1.2 L of CH_3OH results primarily in an adlayer of associatively adsorbed CH_3OH.

The valence features at 8.2 and at 12.6 eV are eliminated by annealing the sample to 150 K. EELS results presented earlier suggest that chemisorbed CH_3OH transforms into adsorbed methoxy by 150 K, and we therefore assign the 6.5 and 10.5 eV features to valance levels of methoxy (i.e., to the $2e$ and $1e/5a_1$ levels, respectively, using C_{3v} classification (36)). Heating to 400 K results in no significant changes in spectral features, suggesting that the majority of surface methoxy species remain intact up to 400 K. EELS, however, shows that there are small changes in the intensity of the methoxy vibrational modes,

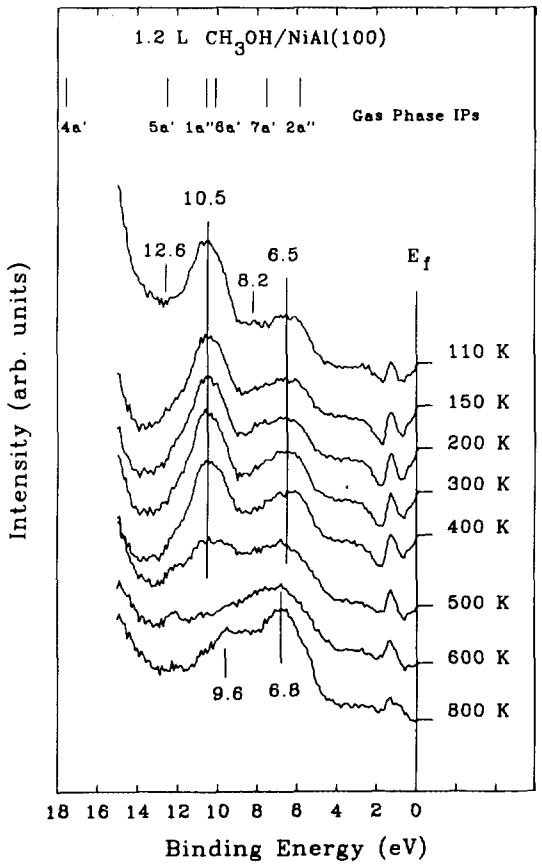

FIG. 10. Difference UPS spectra of CH_3OH/NiAl(100) as a function of temperature. The valence features at 6.5 and 10.5 eV, in the 150–400 K spectra, are associated with surface methoxy. Extensive decomposition of the methoxy adlayer occurs by 500 K. The valence features in the 800 K spectrum are due to the growth of an aluminum oxide layer.

and XPS suggests that carbonaceous fragments develop upon heating from 150 to 400 K. A small amount of methoxy, therefore, decomposes in this temperature range. The 10.5 eV feature, which is believed to be localized in the C–O bond and CH_3 group in methoxy, decreases in intensity, and the 6.5 eV feature is shifted to a new position of 6.8 eV as the surface temperature is raised to 600 K. The change of these spectral features is attributed to the decomposition of a large fraction of methoxy, which results in the desorption of H_2, CH_3 radicals, and C_2H_4, as well as in the deposition of surface oxygen and carbonaceous species. Upon annealing to 800 K, all that remains are two broad features centered at 6.8 and at 9.6 eV, associated with the valence levels of aluminum oxide.

It is now interesting to compare the valence band of methoxy on NiAl(100) and NiAl(110). Figs. 11a and 11b show relevant data (difference spectra) for both surfaces at 300 and 400 K. The positions of the valence levels exhibited in the 300 and 400 K spectra for CH_3OH/NiAl(100) are very similar, suggesting that methoxy changes very little in structure upon heating from 300 to 400 K. There is, however, some decomposition, as was shown by the preceding XPS and EELS results.

Valence band spectra presented in Fig. 11b for CH_3OH/NiAl(110) show something different than the CH_3OH/NiAl(100) spectra. Comparison of the 300 K spectrum of methoxy on NiAl(110) to that of methoxy on NiAl(100) shows that the valence band of methoxy on the (110) face exhibits additional spectral weight near 5.3 eV (highlighted by the crosshatched area). Heating to 400 K results in the loss of this low binding energy feature, as well as a significant decrease in the feature at 10.4 eV, which is presumably associated with the molecular orbital of the C–O bond. We infer from these spectral changes that a significant amount of $CH_3O_{(ad)}$ decomposes between 300 and 400 K on NiAl(110), as has been mentioned in our previous publication. By virtue of the NiA(100) and NiAl(110) comparison, we believe that the 5.3 eV feature is associated with an electronically distinguishable methoxy species that is unique to the (110) plane. We speculate that the presence of Ni in the outermost layer of NiAl(110) is responsible for this species. Unfortunately, whether decomposition of this methoxy species is responsible for the production of methane on NiAl(110) near 350 K cannot be discerned from our data.

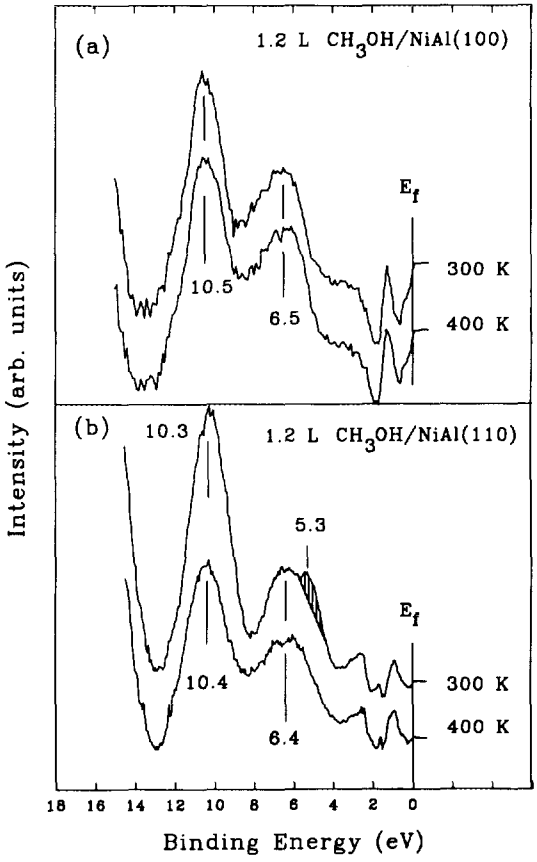

FIG. 11. Difference UPS spectra of (a) CH_3OH/NiAl(100) after exposure to CH_3OH at 120 K and subsequent heating to 300 and 400 K, and (b) CH_3OH/NiAl(110) under the same conditions.

4. SOME GENERAL COMMENTS ON CH_3OH/NiAl(100) AND CH_3OH/NiAl(110)

Results obtained from TPD, XPS, EELS, and UPS and presented in this paper show that the chemisorption and reaction of CH_3OH is sensitive to the atomic composition of the surface. While our results do not allow us to determine whether CH_3OH dissociates to some degree on the NiAl surfaces at 120 K, we can say that at least a fraction adsorbs associatively on both surfaces (at 120 K) at relatively high exposures. By 200 K all the chemisorbed CH_3OH has converted to $CH_3O_{(ad)}$ on both NiAl planes. The structure of the adsorbed adlayer, however, appears to be sensitive to the composition of the alloy surface. As alluded to before, the ν(C–O)/ν(C–H) intensity ratio for $CH_3O_{(ad)}$ is significantly different on the (110) and (100) planes, suggesting that the bonding geometry of this intermediate depends on the relative concentration of Ni and Al in the surface layer. Consistent with this conjecture is that the ν(M–O) mode frequency (640 cm^{-1}) of methoxy on NiAl(100) is about 100 cm^{-1} higher than the frequency of the corresponding mode on the (110) plane (540 cm^{-1}). Also, valence band measurements suggest that the electronic structure of surface-bound methoxy on the (110) plane (at least a fraction thereof) is different than on the (100) face.

Our techniques do not allow us to speculate too much about the bonding of the methoxy intermediate on the NiAl surfaces. With regard to methoxy on NiAl(100), however, we mention that the 640 cm^{-1} mode lies at frequency similar to that of the 655 cm^{-1} ν(M–O) mode of methoxy on monometallic Al(111) (7, 10) and Al(110) (9). This similarity seems to be consistent with prior research that has shown that the outermost layer of the (100) plane is terminated by Al. The ν(C–O)/ν(C–H) intensity ratio, however, is significantly larger on NiAl(100) than on monometallic Al, suggesting that the details of the bonding are different on the alloy and pure metal.

A strong contribution of Al toward the bonding of methoxy on the (110) plane is also expected. As mentioned in the preceding paragraph the ν(M–O) mode of methoxy on the (110) plane is near 540 cm^{-1}, significantly lower than the corresponding mode on monometallic Al. This lower frequency seems to be a result of the presence of both Al and transition metal in the surface layer. We postulate that this may be the case on the basis that a similar mode at 540 cm^{-1} is found for methoxy on the (110) plane of FeAl (37). It is pointed out that while the surface of FeAl may not be a simple ideal termination of the bulk (as it is for NiAl(110)), it does appear that the atomic composition of the surface is made up of both Fe and Al (possibly enriched in Al) (38, 39). Furthermore, the ν(C–O)/ν(C–H) intensity ratio of methoxy on FeAl(110) (37) is very similar to the corresponding ratio for NiAl(110). In the dipole limit this result suggests that methoxy may be further tilted away from the surface normal on the (110) planes of NiAl and FeAl than on NiAl(100).[5] It is not clear, however, what the ramifications of this different bonding scheme on the (110) plane is, since within the resolution of our EELS, XPS, and UPS experiments, the temperature range for methoxy decomposition is similar on both NiAl(110) and NiAl(100).

The effect of Ni in the outermost layer of the NiAl alloy also is shown in part by the TPD results. While methoxy appears to decompose between 300 and 400 K on both the (100) and (110) planes, only on the latter plane does a significant amount of methane desorb in this temperature interval. Presumably, the hydrogenation capabilities of monometallic Ni are retained to some degree in the alloy and are able to remove hydrocarbon fragments from the alloy as methane. This reaction channel appears to be very limited on the (100) surface, as evidenced by the very little CH_4 desorption (relative to NiAl(110)) and by XPS results which show that the concentration of surface carbon is constant, within experimental error, between 300 and 400 K. Ni also exerts an influence on the desorption of products between 400 and 500 K, since CO desorbs from NiAl(110), but it is not evolved from the Al-terminated (100) surface. The production of CO on the (110) plane, however, appears to be limited by the decomposition rate of methoxy, while on monometallic Ni the evolution of CO from methoxy decomposition is limited by its own desorption kinetics. We base this contention for CH_3OH/NiAl(110) largely on the fact that a relatively intense C–O stretching mode near 2000 cm^{-1}, characteristic of adsorbed CO, does not appear in our EELS data in any temperature interval.

Above 500 K the decomposition behavior of methoxy and coadsorbed decomposition fragments on NiAl(110) and NiAl(100) is similar. Aside from the deposition of copious amounts of surface oxygen and carbonaceous species, the desorption of methyl occurs at 570 K on both planes of NiAl.[6,7] Theoretical calculations suggest that the dehydrogenation of methoxy on metal surfaces will be suppressed in the presence of coadsorbed oxygen (40). With this in mind, it is suspected that coadsorbed oxygen (and carbonaceous fragments) also suppresses the dehydrogenation of methoxy on the NiAl alloy surfaces so that the intermediate can exist to temperatures where methyl desorption can become an operative reaction step. Fi-

[5] Recent results in our laboratory show that the relative intensities of the methoxy modes for FeAl(100) are very similar to those for methoxy on NiAl(100).

[6] Methyl radical desorption is also found during methoxy decomposition on O/Mo(110); see Serafin, J. G., and Friend, C. M., *J. Am. Chem. Soc.* **111**, 8967 (1989).

[7] Theoretical treatment of methyl ejection from methoxy on O/Mo(110) Ref. (44) suggests that the C–O bond strength in methoxy on Mo is about 1.4 eV; see Shiller, P., and Anderson, A. B., *J. Phys. Chem.* **95**, 1396 (1991).

nally, it is pointed out that surface segregation and the oxidation of Al probably results in the atomic composition of the (110) and (100) planes being very similar above 500 K, which is consistent with the similarity in the peak temperature of methyl radical desorption from CH_3OH/NiAl(110) and CH_3OH/NiAl(110).[8]

5. SUMMARY

Methanol adsorption and thermal decomposition on the (100) and (110) surfaces of stoichiometric NiAl have been compared on the basis of TPD, XPS, UPS, and EELS data. At a temperature of 120 K, the majority of methanol associatively chemisorbs on NiAl(100), forming a mixed layer of methoxy, atomic hydrogen, and methanol, while methanol chemisorption on NiAl(110) is associative. H_2, CH_3, CH_4, and small amounts of C_2H_4 are found to desorb from both surfaces but the production of gaseous CO is unique to the NiAl(110) face. Also, the majority of the surface hydrogen, which results from O–H bond cleavage, combines and desorbs from NiAl(100) at a peak temperature of 260 K, which is 80 K lower than the corresponding desorption temperature of hydroxyl-hydrogen from the (110) plane. The difference in the chemical reactivities of these two surfaces toward methanol decomposition is primarily attributed to their different surface atomic composition and structure. The production of CH_4 near 350 K via hydrogenation reactions and CO at 440 K on NiAl(110) is believed to be facilitated by the presence of Ni atoms in the outermost layer. In contrast, on NiAl(100), where only Al resides in the outermost layer, no oxygenated species desorb and hydrogenation reactions are almost completely suppressed. The desorption of CH_3 radicals occurs from both surfaces with a peak temperature of 570 K. This product is thought to be due to the homolysis of the C–O bond of $CH_3O_{(ad)}$ bound preferentially on Al or its oxide.

6. ACKNOWLEDGMENTS

Partial support of this research by the National Science Foundation through an NSF-NYI award is appreciated (Grant DMR-925844). We also appreciate Dr. Ram Darolia, at General Electric Aircraft Engines, for supplying a single crystal ingot of NiAl.

REFERENCES

1. Nieuwenhuys, B. E., *in* "The Chemical Physics of Solid Surfaces" (D. A. King and D. P. Woodruff, Eds.), Vol. 6, p. 185. Elsevier, Amsterdam, 1993.
2. Davis, H. L., and Noonan, J. R., *Phys. Rev. Lett.* **54,** 566 (1985).
3. Yalisove, S. M., and Graham, W. R., *Surf. Sci.* **183,** 556 (1987).
4. Davis, H. L., and Noonan, J. R., *in* "Physical and Chemical Properties of Thin Metal Overlayers and Alloy Surfaces" (D. M. Zehner and D. W. Goodman, Eds.), Vol. 83, p. 3. Mater. Res. Soc., Pittsburgh, PA, 1987.
5. Wise, H., and Oudar, J., "Material Concepts in Surface Reactivity and Catalysis," p. 113. Academic Press, San Diego, 1990.
6. Sheu, B.-R., Chaturvedi, S., and Strongin, D. R., *J. Phys. Chem.* **98,** 10258 (1994).
7. Chen, J. G., Basu, P., Ng., L., and Yates, J. T., Jr., *Surf. Sci.* **194,** 397 (1988).
8. Rogers, J. W., Hance, R. L., Jr., and White, J. M., *Surf. Sci.* **100,** 388 (1980).
9. Tindall, I. F., and Vickerman, J. C., *Surf. Sci.* **149,** 577 (1985).
10. Basu, P., Chen, J. G., Ng, L. I., Colaianni, M. L., and Yates, J. T., Jr., *J. Chem. Phys.* **89,** 2406 (1988).
11. Waddill, G. D., and Kesmodel, L. L., *Surf. Sci.* **182,** L248 (1987).
12. Vajo, J., Campbell, J. H., and Becker, C. H., *J. Phys. Chem.* **95,** 9457 (1991).
13. Vajo, J., Campbell, J. H., and Becker, C. H., *J. Vac. Sci. Technol. A* **7,** 1949 (1989).
14. Richter, L. J., Gurney, B. A., Villarrubias, J. S., and Ho, W., *Chem. Phys. Lett.* **113,** 185 (1984).
15. Richter, L. J., and Ho, W., *J. Chem. Phys.* **83,** 2569 (1985).
16. Richter, L. J., and Ho, W., *J. Vac. Sci. Technol. A* **3,** 1549 (1985).
17. Bare, S. R., Stroscio, J. A., and Ho, W., *Surf. Sci.* **150,** 399 (1985).
18. Johnson, S., and Madix, R. J., *Surf. Sci.* **103,** 361 (1981).
19. Hall, R. B., Desantolo, A. M., and Bare, S. J., *Surf. Sci.* **161,** L533 (1985).
20. Miragliotta, J., Polizzotti, R. S., Rabinowitz, P., Cameron, S. D., and Hall, R. B., *Chem. Phys.* **143,** 123 (1990).
21. Madix, R. J., Lee, S. B., and Thornburg, M. J., *J. Vac. Sci. Technol. A* **1,** 1254 (1983).
22. Baudais, F. L., Borschke, A. J., and Dignam, M. J., *Surf. Sci.* **100,** 210 (1980).
23. Gates, S. M., Russell, J. N., and Yates, J. T., Jr., *Surf. Sci.* **159,** 233 (1985).
24. Gates, S. M., Russell, J. N., and Yates, J. T., Jr., *J. Catal.* **92,** 25 (1985).
25. Gates, S. M., Russell, J. N., and Yates, J. T., Jr., *Surf. Sci.* **146,** 199 (1984).
26. Demuth, J. E., and Ibach, H., *Chem. Phys. Lett.* **60,** 395 (1979).
27. Hall, R. B., De Santolo, A. M., and Grubb, S. G., *J. Vac. Sci. Technol. A* **5,** 865 (1987).
28. Rubloff, G. W., and Demuth, J. E., *J. Vac. Sci. Technol. A* **14,** 419 (1977).
29. Russell, J. N., Chorkendorff, I., and Yates, J. T., Jr., *Surf. Sci.* **183,** 316 (1987).
30. Chen, B., and Falconer, J. L., *J. Catal.* **144,** 214 (1993).
31. Lin, J.-L., and Bent, B. E., *J. Am. Chem. Soc.* **115,** 2849 (1993).
32. Serafin, J. G., and Friend, C. M., *J. Am. Chem. Soc.* **111,** 8967 (1989).
33. Creighton, J. R., *Surf. Sci.* **234,** 287 (1990).
34. Sheu, B.-R., and Strongin, D. R., *J. Phys. Chem.* **97,** 10144 (1993).
35. Robin, M. B., and Kuebler, N. A., *J. Electron Spectrosc. Relat. Phenom.* **1,** 13 (1972/73).
36. Witko, M., Hermann, K., Ricken, D., Stenzel, W., Conrad, H., and Bradshaw, A. M., *Chem. Phys.* **177,** 363 (1993).
37. Sheu, B.-R., and Strongin, D. R., *Langmuir* **10,** 1801 (1994).
38. Graupner, H., and Zehner, D. M., private communication.
39. Gleason, N. R., and Strongin, D. R., in preparation.
40. Shiller, P., and Anderson, A. B., *J. Phys. Chem.* **97,** 189 (1993).

[8] Calculations suggest that methyl ejection from methoxy on oxidized Al is energetically possible at elevated temperatures. See Anderson, A. B., and Jen, S. -F., *J. Phys. Chem.* **95,** 7792 (1991).